Disruption of forkhead transcription factor (FOXO) family members in mice reveals their functional diversification

Taisuke Hosaka*†, William H. Biggs III*†‡, David Tieu*, Antonia D. Boyer*, Nissi M. Varki§, Webster K. Cavenee*§¶‖, and Karen C. Arden*§¶**

*Ludwig Institute for Cancer Research, §Department of Medicine, ¶Cancer Center, and ‖Center for Molecular Genetics, University of California at San Diego, La Jolla, CA 92093-0660

Communicated by Raymond L. White, University of California at San Francisco, Emeryville, CA, January, 6, 2004 (received for review October 12, 2003)

Genetic analysis in *Caenorhabditis elegans* has uncovered essential roles for DAF-16 in longevity, metabolism, and reproduction. The mammalian orthologs of DAF-16, the closely-related FOXO subclass of forkhead transcription factors (FKHR/FOXO1, FKHRL1/FOXO3a, and AFX/FOXO4), also have important roles in cell cycle arrest, apoptosis and stress responses *in vitro*, but their *in vivo* physiological roles are largely unknown. To elucidate their role in normal development and physiology, we disrupted each of the *Foxo* genes in mice. *Foxo1*-null embryos died on embryonic day 10.5 as a consequence of incomplete vascular development. *Foxo1*-null embryonic and yolk sac vessels were not well developed at embryonic day 9.5, and *Foxo1* expression was found in a variety of embryonic vessels, suggesting a crucial role of this transcription factor in vascular formation. On the other hand, both *Foxo3a*- and *Foxo4*-null mice were viable and grossly indistinguishable from their littermate controls, indicating dispensability of these two members of the Foxo transcription factor family for normal vascular development. *Foxo3a*-null females showed age-dependent infertility and had abnormal ovarian follicular development. In contrast, histological analyses of *Foxo4*-null mice did not identify any consistent abnormalities. These results demonstrate that the physiological roles of *Foxo* genes are functionally diverse in mammals.

The FOXO subclass of the forkhead box transcription factors is evolutionarily conserved, and its origin may predate the divergence of the vertebrate and invertebrate lineage (1). Genetic analysis has shown that the insulin-signaling pathway negatively regulates DAF-16, the *Caenorhabditis elegans* ortholog of Foxo (2, 3), and modulates the lifespan, metabolism, and fertility of the worm (4). Activation of insulin signaling pathways in mammals also negatively regulates members of the FOXO transcription factors (FOXO1/FKHR, FOXO3a/FKHRL1, and FOXO4/AFX) through direct phosphorylation of three conserved residues by the Akt (PKB) serine/threonine kinase, resulting in their active nuclear export and thereby inhibition of their transcriptional activities (5–8). Several *in vitro* overexpression studies have suggested that *FOXO* genes play important roles in several biological processes such as control of the cell cycle, apoptosis, and stress response, and some shared downstream transcriptional targets have been identified (9, 10). However, each *FOXO* gene has a unique pattern of expression in tissues (11–14) and exhibits a distinct response under a variety of conditions (15–17), suggesting that their *in vivo* physiological roles might be different. To test this, we disrupted each of the three *Foxo* genes in mice. We have previously shown that *Foxo1* haploinsufficiency restores insulin sensitivity and rescues the diabetic phenotype in insulin-resistant mice (18). Here, we describe the phenotype of mice completely lacking each *Foxo* gene. Our results demonstrate that the physiological roles of *Foxo* genes are quite diverse in mammals.

Materials and Methods

Mutant Mice. Generation of the targeted *Foxo1* allele has been described (18). The mice are maintained as heterozygotes and homozygous embryos were obtained by intercrossing. *Foxo3a* mutant mice were generated by using embryonic stem (ES) cell clones from OmniBank(R) ES cell library of randomly targeted cell lines (Lexicon Genetics, The Woodlands, TX) (19). The gene trap vector was inserted into the *Foxo3a* intron 1 as shown schematically in Fig. 4. Targeted 129/SvEvBrd-derived ES cells were injected into C57BL/6 blastocysts. The chimeric male was crossed with C57BL/6 females to generate the heterozygotes, and heterozygotes were crossed to generate the homozygotes. The *Foxo4* targeting vector contained 6.5 kb of genomic sequence immediately 5′ side of the first exon followed by a 1.3-kb phosphoglycerate kinase promoter-driven neomycin phosphotransferase (PGK-Neo) cassette and 1.5 kb of genomic sequence of intron 1. The *Foxo4* targeting vector also had a polyoma enhancer/herpes simplex virus thymidine kinase (MC1-TK) cassette for negative selection. The targeting vector was linearized and electroporated into 129/SvJ-derived ES cells. G418-resistant ES clones were screened for homologous recombination by Southern blot analysis and injected into C57BL/6 blastocysts. Because the *Foxo4* locus is located on the X chromosome, the chimeric male was crossed with C57BL/6 females to generate the heterozygous females or hemizygous males, which were subsequently crossed to generate homozygous females. All protocols used in this study were approved by the Animal Subjects Program of the University of California at San Diego and conformed to National Institute of Health guidelines and public law. All mice were maintained on a 12-h light/dark cycle with food and water provided ad libitum.

Genotyping. DNA from tails was analyzed by Southern blotting. *Foxo1* genotyping has been described (18). *Foxo3a* genotyping was performed by comparing autoradiographic intensities of 1.5-kb *Sac*I fragments hybridized to a Neo-specific probe as described (20). The *c-src* tyrosine kinase (*Csk*)-specific probe was used as a control for copy number. This strategy discriminates zero-, one-, or two-targeted gene disruptions, representing +/+, +/−, and −/− mice, respectively, at any trapped genetic locus. For *Foxo4* genotyping, *Bam*HI-digested DNA was hybridized with a probe from the 3′ region of *Foxo4* cDNA. To genotype the *Foxo1* mutant embryo and yolk sac, genomic DNA from small portions of embryo or yolk sac were analyzed by PCR. Primers used for genotyping were 5′-TGG GAG CCC TGA AGT GAG TA-3′ (primer 1), 5′-ATG TCC CAC CTG TGA TTC TG-3′ (primer 2), and 5′-CCA TCA TGG CTG ATG CAA TG-3′ (primer 3). Primers 1 and 2 amplified 301-bp fragments

Abbreviations: E*n*, embryonic day *n*; ES, embryonic stem.

†T.H. and W.H.B. contributed equally to this work.

‡Present address: Ambit Biosciences, 9875 Towne Centre Drive, San Diego, CA 92122.

**To whom correspondence should be addressed at: Ludwig Institute for Cancer Research, 9500 Gilman Drive, La Jolla, CA 92093. E-mail: karden@ucsd.edu.

GENETICS

from the wild-type *Foxo1* allele. Primers 2 and 3 amplified 815-bp fragments from the mutant allele.

Northern Blot Analysis. Total RNA was prepared from skeletal muscle of wild-type and *Foxo4*-null mice by using TRIzol (Invitrogen). Ten micrograms of total RNA was electrophoresed through 1% agarose gels, transferred to Hybond-N+ membranes (Amersham Biosciences), and hybridized to a probe from the 3′ region of *Foxo* cDNA.

Western Blot Analysis. Twenty micrograms of lysate were prepared from tissues from both wild-type and *Foxo1*-null embryonic day (E) 9.5 embryos and wild-type and *Foxo3a*-null adult mice, separated by electrophoresis, and blotted to nitrocellulose membranes. Antibodies used for Western analysis were polyclonal anti-FKHR antibody (C-20, Santa Cruz Biotechnology), polyclonal anti-FKHRL1 antibody (Upstate Biotechnology, Waltham, MA), monoclonal anti-β-actin antibody (clone AC-15, Sigma), and horseradish peroxidase (HRP)-conjugated secondary antibodies (Dako).

Immunohistochemistry of Whole-Mount Embryos and Yolk Sacs. Embryos and yolk sacs were fixed overnight in 4% paraformaldehyde/PBS and bleached with 5% H_2O_2 in methanol for 5 h. Staining, washing, and developing procedures were essentially the same as described (21). Antibodies used for immunohistochemistry were the monoclonal anti-PECAM-1 antibody (clone MEC 13.3, BD Pharmingen) and HRP-conjugated secondary antibodies (Jackson ImmunoResearch).

LacZ Staining. Whole-mount embryo or yolk sac tissues were fixed in 0.25% glutaraldehyde/PBS for 10 min, rinsed three times with PBS, and stained overnight at 37°C with X-Gal buffer (5 mM potassium ferrocyanide/5 mM potassium ferricyanide/1 mM magnesium chloride/0.2% Triton X-100/1 mg/ml X-Gal in PBS, pH 7.3). For lacZ staining of sections, embryos were fixed in 4% paraformaldehyde/PBS at 4°C for 1 h and equilibrated with 30% sucrose/PBS at 4°C. Embryos were then embedded in OCT compound, cryosectioned, and stained with X-Gal buffer. After lacZ staining, samples were counterstained by nuclear fast red. Some tissues were cryosectioned after whole-mount lacZ staining.

Histological Analysis. Tissues embedded in paraffin were sectioned and stained with hematoxylin/eosin. The tissues that were examined for initial screening of *Foxo3a*- and *Foxo4*-null animals were white and brown adipose tissue, adrenal glands, femur, sternum, brain, reproductive tract, clitoral glands, eyes, Harderian glands, gastrointestinal tract, liver with gall bladder, heart, kidneys, lung, mesenteric lymph node, mammary gland, skin, pancreas, salivary gland, skeletal muscle, spinal cord, spleen, thymus, thyroid gland, trachea, urinary bladder from females, testes, epididymides, kidneys, preputial glands, prostate, salivary gland, seminal vesicles, and coagulating gland from males. A board-certified veterinary pathologist (American College of Veterinary Pathologists) at the Charles River Laboratory performed the initial examination of all histological sections. A detailed analysis of the ovarian phenotype in the *Foxo3a*-null mice was performed in conjunction with the University of California at San Diego Cancer Center Core Histology facility. Histology of mouse ovarian follicles was categorized by the standard classification (22).

Results

***Foxo1* Is Required for Embryonic Vascular Development.** While generating mice with *Foxo1* haploinsufficiency to test its role in insulin sensitivity, we noticed the absence of homozygous *Foxo1*$^{-/-}$ mice in litters derived from heterozygous matings

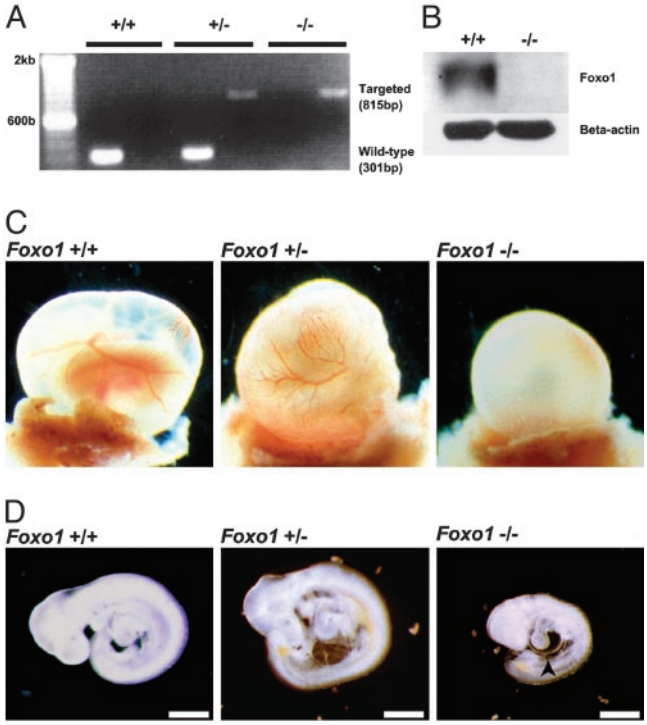

Fig. 1. Disruption of the *Foxo1* gene results in embryonic lethality. (*A*) PCR analysis with genomic DNA from E9.5 yolk sacs obtained from a mating of *Foxo1*$^{+/-}$ mice. PCR amplification from the wild-type and *Foxo1*-targeted loci resulted in fragment sizes of 301 bp and 815 bp, respectively. Samples were independently amplified with each primer set. (*B*) Western blot analysis of lysates from E9.5 *Foxo1*$^{+/+}$ and *Foxo1*$^{-/-}$ embryos by using antibodies against Foxo1 and β-actin. (*C*) At E9.5, both *Foxo1*$^{+/+}$ and *Foxo1*$^{+/-}$ yolk sacs had well developed blood vessels, whereas *Foxo1*$^{-/-}$ yolk sacs lacked them. (*D*) At E9.5, *Foxo1*$^{+/+}$ and *Foxo1*$^{+/-}$ embryos were phenotypically indistinguishable in appearance, whereas *Foxo1*$^{-/-}$ embryos were approximately half their size. In addition, cardiac looping was retarded and the pericardium was distended (arrowhead). (Scale bar, 500 μm.)

suggesting that *Foxo1*$^{-/-}$ animals were unable to complete embryonic development (18). To address this possibility, embryos were isolated from timed matings, and their genotypes and Foxo1 expression levels were assessed by genomic PCR and Western analyses, respectively (Fig. 1 *A* and *B*). At E9.5, there was no apparent difference between *Foxo1*$^{+/+}$ and *Foxo1*$^{+/-}$ yolk sacs, but *Foxo1*$^{-/-}$ yolk sacs lacked well developed blood vessels (Fig. 1*C*). *Foxo1*$^{+/+}$ and *Foxo1*$^{+/-}$ embryos were also phenotypically indistinguishable in appearance, whereas *Foxo1*$^{-/-}$ embryos were ≈50% the size of their *Foxo1*$^{+/+}$ littermates (Fig. 1*D*). Furthermore, cardiac looping of *Foxo1*$^{-/-}$ embryos was retarded and the pericardium was distended compared to *Foxo1*$^{+/+}$ and *Foxo1*$^{+/-}$ embryos at E9.5. Despite these developmental defects, the hearts of *Foxo1*$^{-/-}$embryos were still beating at E9.5. However, none of them survived beyond E10.5.

We next examined the vascular structures of *Foxo1*$^{-/-}$ embryos and yolk sacs and compared them with control littermates by whole-mount immunostaining with a monoclonal antibody to PECAM-1, a specific marker for vascular endothelial cells. Significant defects in the formation of the vascular system were observed in *Foxo1*$^{-/-}$ embryos compared to those of *Foxo1*$^{+/+}$ (Fig. 2*A*). The dorsal aorta in *Foxo1*$^{-/-}$ embryos appeared thin and disorganized (Fig. 2 *A* and *B*), and the intersomitic vessels in *Foxo1*$^{-/-}$ embryos were also irregularly developed (Fig. 2*B*). The vasculature in the heads of *Foxo1*$^{-/-}$ embryos appeared to lack properly formed branches of the internal carotid artery (Fig. 2*C*). In addition, developed vasculature was not present in

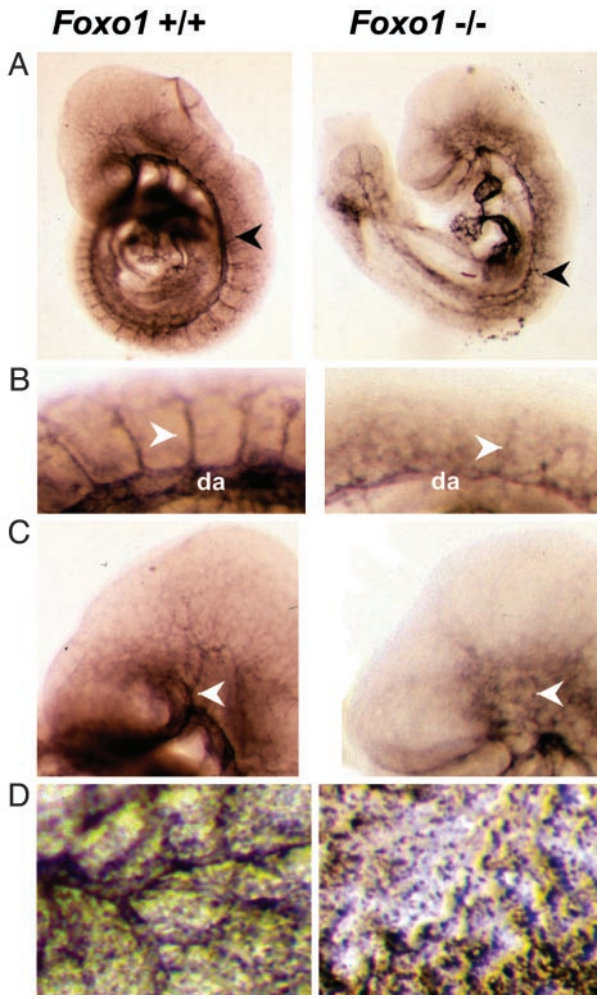

Fig. 2. Foxo1$^{-/-}$ embryos and yolk sacs show defective vascular development. (*A*) PECAM-1 immunostaining of whole-mount E9.5 *Foxo1*$^{+/+}$ and *Foxo1*$^{-/-}$ embryos, respectively. Note the thin and disorganized dorsal aorta in *Foxo1*$^{-/-}$ embryo compared with *Foxo1*$^{+/+}$ embryo (arrowheads). (*B*) Magnified view of the E9.5 *Foxo1*$^{+/+}$ and *Foxo1*$^{-/-}$ intersomitic vessels. Intersomitic vessels in *Foxo1*$^{-/-}$ embryo were disorganized compared with *Foxo1*$^{+/+}$ (arrowheads). da, dorsal aorta. (*C*) Magnified view of the E9.5 *Foxo1*$^{+/+}$ and *Foxo1*$^{-/-}$ head vessels. The vessels of the head, including the branches of the internal carotid artery, were properly developed in *Foxo1*$^{+/+}$ but not in *Foxo1*$^{-/-}$ embryos (arrowheads). (*D*) PECAM-1 staining of *Foxo1*$^{+/+}$ and *Foxo1*$^{-/-}$ yolk sacs. Properly developed vasculature was present in *Foxo1*$^{+/+}$ yolk sacs but not in *Foxo1*$^{-/-}$ yolk sacs.

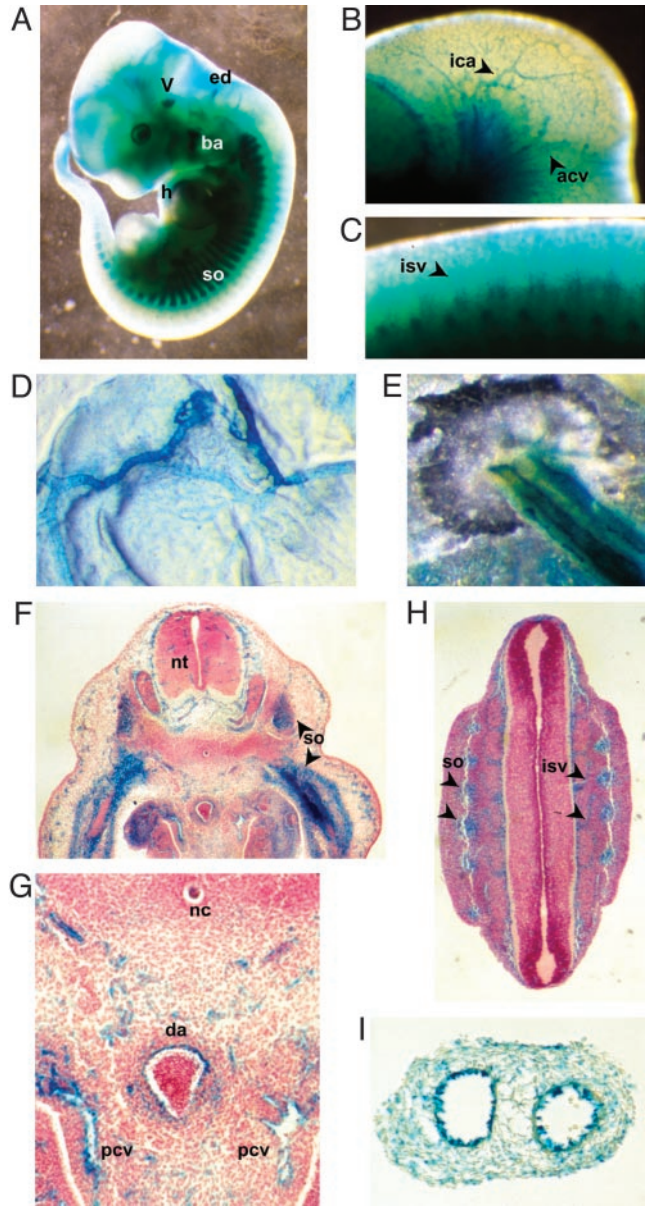

Fig. 3. LacZ expression from the insertional targeting vector in heterozygous *Foxo*$^{+/-}$ embryos and extraembryonic tissues at E11.5. (*A*) Whole-mount lacZ staining of embryo. LacZ was expressed in several tissues such as the somites (so), branchial arch (ba), heart (h), endolymphatic diverticulum of otocyst (ed), and trigeminal ganglia (V). (*B* and *C*) Magnified view of the lacZ stained head and trunk, respectively. Lac Z staining was found in branches of the internal carotid artery (ica), anterior cardinal vein (acv), and intersomitic vessels (isv). (*D* and *E*) Whole-mount lacZ staining of the yolk sac and umbilical cord, respectively. Both vitelline vessels and both umbilical vessels were stained. (*F–H*) LacZ staining for sectioned E11.5 embryo. Various vessels including the capillaries in the neural tube (nt), dorsal aorta (da), posterior cardinal vein (pcv) and intersomitic vessels (isv) were stained. (*G*) Magnified view of *F*. so, somite; nc, notocord. (*I*) Section of lacZ-stained umbilical cord. The endothelial layers of the two vessels (common umbilical artery and vein) were stained.

Foxo1$^{-/-}$ yolk sacs (Fig. 2*D*). Thus, the primary defect in *Foxo1*$^{-/-}$ embryos and yolk sacs appears to be a disruption of normal vascular formation.

The targeting construct we used to disrupt the *Foxo1* gene included a promoterless lacZ gene (18), allowing *Foxo1* promoter activity (i.e., normal *Foxo1* expression) to be monitored by surrogate lacZ staining (14). In whole-mount heterozygous *Foxo1*$^{+/-}$ embryos, lacZ staining was observed in several tissues and organs such as head vasculature, somite, branchial arch, heart, trigeminal ganglia, and the endolymphatic diverticulum of otocyst (Fig. 3*A*). A magnified view showed that branches of the internal carotid artery and anterior cardinal vein in the head and intersomitic vessels in the trunk were also stained (Fig. 3 *B* and *C*). In addition, the extraembryonic vasculature including the vitelline and umbilical vessels were stained (Fig. 3 *D* and *E*). To examine the precise location of expression, we performed lacZ staining on cryosectioned *Foxo1*$^{+/-}$ embryos at E11.5. Staining was apparent in the somites (Fig. 3 *F* and *H*) and endothelium of variously sized vessels, including the capillaries in the neural tube (Fig. 3*F*), the dorsal aorta, the posterior cardinal veins (Fig. 3*G*), and the intersomitic vessels (Fig. 3*H*). The endothelia of both the common umbilical artery and vein stained for lacZ (Fig. 3*I*). These results indicate that *Foxo1* is highly expressed in developing embryonic vasculature.

GENETICS

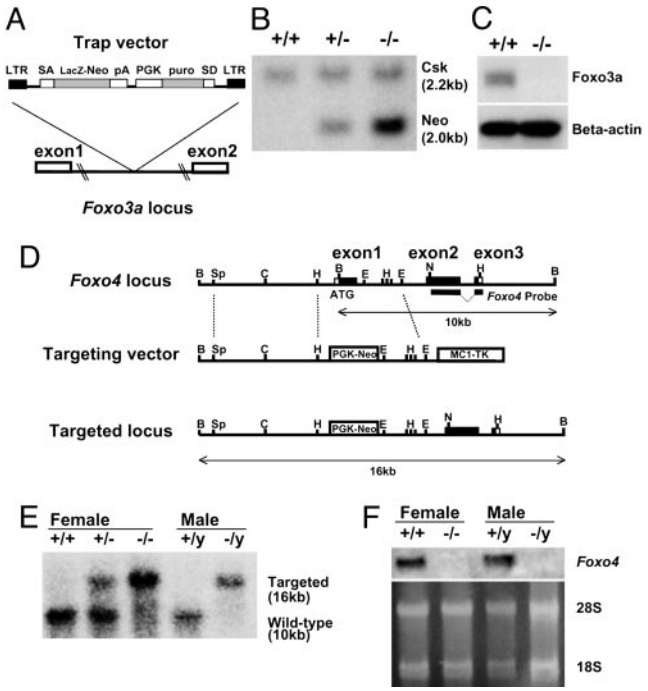

Fig. 4. Targeted disruption of the *Foxo3a* gene and *Foxo4* gene. (*A*) Targeting strategy for *Foxo3a*. A retroviral promoter trap vector was inserted in intron 1 of *Foxo3a*. SA, splice acceptor site; SD, splice donor site; LTR, long terminal repeat sequence; pA, polyadenylation signal; puro, puromycin. (*B*) Southern analysis of *Sac*I-digested genomic DNA obtained from a mating of *Foxo3a*$^{+/-}$ mice by using the *Neo*- and *Csk*-specific probes. Different intensities demonstrated by hybridization of the Neo-specific probe discriminate zero, one, or two *Foxo3a* gene disruptions, representing +/+, +/−, and −/− mice, respectively. (*C*) Western analysis of lung tissue lysates from *Foxo3a*$^{+/+}$ and *Foxo3a*$^{-/-}$ mice by using antibodies against Foxo3a and β-actin. (*D*) Restriction maps of the wild-type *Foxo4* locus, the targeting vector, and the targeted locus. The targeting vector contained a *PGK-Neo* cassette instead of the *Foxo4* exon1. A targeting probe (3′ region of *Foxo4* cDNA) was also indicated. Restriction enzymes were indicated as B, *Bam*HI; C, *Cla*I; E, *Eco*RI; H, *Hin*dIII; N, *Nco*I; and Sp, *Spe*I. (*E*) Southern analysis of *Bam*HI-digested genomic DNA obtained from *Foxo4* female (+/+, +/−, and −/−) and male (+/y and −/y) mice by using a probe from the 3′ region of *Foxo4* cDNA. The *Foxo4* wild-type allele (10 kb) and targeted allele (16 kb) were indicated. (*F*) Northern analysis of total RNA from skeletal muscle of *Foxo4* female (+/+ and −/−) and male (+/y and −/y) mice by using the same probe used for Southern blot analysis. The ethidium bromide-staining 28S and 18S bands are also indicated.

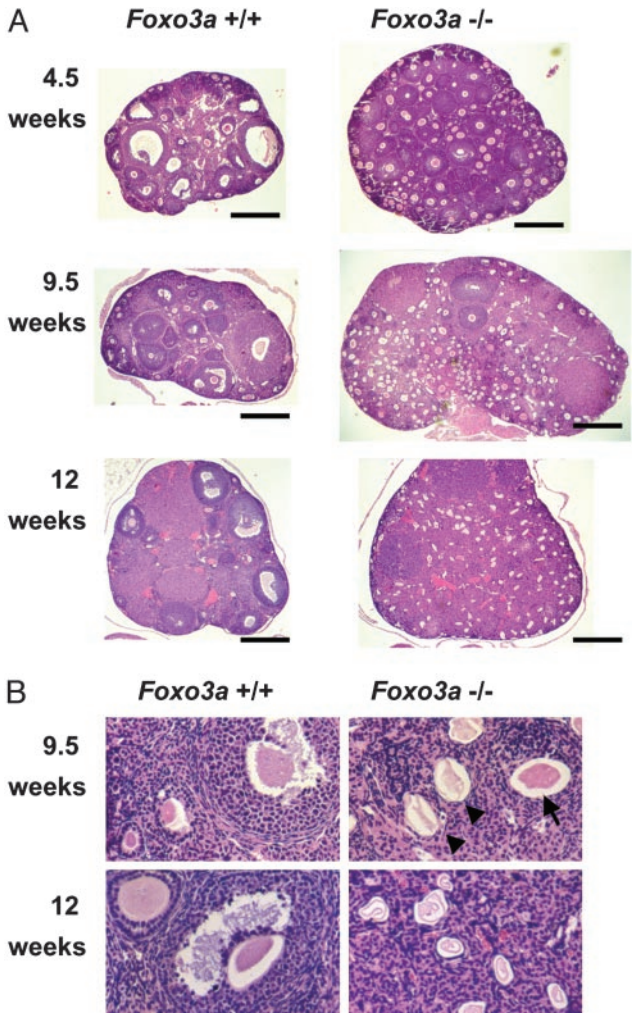

Fig. 5. Histological analysis of ovaries with hematoxylin/eosin staining. (*A*) At 4.5 weeks of age, developing follicles containing growing oocytes but no antrums (type 3b-5b) were prominent, but mature follicles containing antrums (type 6–7) were less common in *Foxo3a*$^{-/-}$ ovaries. At 9.5 weeks of age, *Foxo3a*$^{-/-}$ ovaries had many developing follicles and few mature follicles, similar to those at 4.5 weeks. At 12 weeks of age, *Foxo3a*$^{-/-}$ ovaries had no developing follicles, and all oocytes had undergone degeneration. Each specimen was sectioned at its largest diameter. (Scale bar, 500 μm.) (*B*) Various stages of follicles were found in wild-type ovaries at both 9.5 and 12 weeks of age. Normal oocytes (arrow) were present, but degenerating oocytes (arrowheads) were prominent in *Foxo3a*$^{-/-}$ ovaries at 9.5 weeks of age. All oocytes had undergone degeneration in *Foxo3a*$^{-/-}$ ovaries at 12 weeks of age.

***Foxo3a* Is Required for Ovarian Follicular Development, Whereas *Foxo4*$^{-/-}$ Mice Are Grossly Normal in Appearance.** To explore the *in vivo* roles of other *Foxo* members, we generated mice with disruptions of either *Foxo3a* or *Foxo4*. Disruption of *Foxo3a* was accomplished by retroviral-mediated gene trapping within intron 1 (Fig. 4*A*). Progeny were genotyped by quantitative Southern blot analysis (Fig. 4*B*; see *Materials and Methods*) and the resultant lack of Foxo3a expression was confirmed by Western blot analysis (Fig. 4*C*). Disruption of *Foxo4* was accomplished by homologous gene targeting (Fig. 4*D*). Genotyping was performed by Southern blot analysis (Fig. 4*E*) and lack of *Foxo4* expression was determined by Northern blot analysis (Fig. 4*F*). In contrast to *Foxo1*-null mice, both *Foxo3a*- and *Foxo4*-null mice were viable, born with the predicted Mendelian frequencies and grossly indistinguishable from their wild-type littermates. Histological analysis of >30 tissues (see *Materials and Methods*) from *Foxo3a*-null, *Foxo4*-null, and their normal counterparts at ≈9 weeks of age revealed no consistent histological difference among them with one exception. The ovaries from *Foxo3a*$^{-/-}$ female mice were clearly abnormal (see below). *Foxo3a*$^{-/-}$ females were completely sterile when mated at the age of 10 weeks or more ($n = 9$), while being fertile when mated at the age of 7 weeks or less ($n = 4$). On the other hand, *Foxo4*$^{-/-}$ males and females, as well as *Foxo3a*$^{-/-}$ males, showed no impairment of reproductive fitness. Further histological analysis of *Foxo3a*$^{-/-}$ ovaries showed abnormal follicular development (Fig. 5). At 4.5 weeks of age (i.e., the onset of puberty), developing follicles containing growing oocytes but no antrum (type 3b-5b) were more prominent, but mature follicles, containing antrum (type 6–7), were much less common in *Foxo3a*$^{-/-}$ ovaries than in *Foxo3a*$^{+/+}$ ovaries (Fig. 5*A*). At 9.5 weeks of age, *Foxo3a*$^{-/-}$ ovaries contained plenty of developing follicles and only a few mature follicles compared to *Foxo3a*$^{+/+}$ ovaries, similar in appearance to those observed at 4.5 weeks (Fig. 5*A*). The most prominent finding in *Foxo3a*$^{-/-}$ ovaries at 9.5 weeks was that the considerable number of oocytes in developing

follicles had appeared to have undergone degeneration, indicating initiation of atretic change (Fig. 5*B*). At 12 weeks of age, *Foxo3a*$^{-/-}$ ovaries had no developing follicles and all oocytes present had undergone degeneration (Fig. 5). As *Foxo3a*$^{+/-}$ females were fertile and their ovaries were histologically indistinguishable from wild-type ovaries (data not shown), the presence of one *Foxo3a* allele appears to be sufficient for the normal regulation of ovarian follicular development.

Discussion

Here we showed that *Foxo1* is expressed in developing embryonic vasculature and complete disruption of *Foxo1* resulted in embryonic lethality due to vascular defects. Thus, Foxo1 is an essential regulator in embryonic vessel formation. Formation of the embryonic vasculature has been separated into two major processes, vasculogenesis and angiogenesis (23). During the initial stages of vascular development, endothelial cell precursors form a network of homogeneous and primitive blood vessels (the primary vascular plexus) by the process of vasculogenesis. The primary vascular plexus is then remodeled through the process of angiogenesis by sprouting and pruning blood vessels and recruiting mural cells to establish the vascular structure. In *Foxo1*-null mutant embryos, vasculature stained by PECAM-1 can be seen at E9.5, although it is immature compared to wild-type embryos. This finding suggests that Foxo1 may not have a major role in the process of embryonic vasculogenesis. However, the failure to establish normal vasculature in *Foxo1*-null embryos indicates that Foxo1 plays an important role in the process of embryonic angiogenesis.

Our results raise several interesting questions related to the molecular mechanisms of Foxo1 regulation in vascular development. First, which signaling pathways regulate Foxo1? Studies in *C. elegans* have revealed that the regulation of DAF-16 by DAF-2 signaling modulates several physiological reactions (2–4). Because *C. elegans* is devoid of a vascular circulatory system, the role of Foxo1 in this system cannot be inferred from its study. It is also unclear whether the focused regulation of Foxo1 by insulin signaling is conserved in mammalian vascular development. In fact, other receptor tyrosine kinase signaling, such as those involved with the VEGF, PDGF, angiopoietin, and EphrinB pathways might be expected to have more direct roles in physiological vessel formation than insulin/IGF signaling (23). Second, how does the phosphorylation status of Foxo1 in vessels change during vascular development? A recent report showed that increased phosphorylation of Foxo1 is associated with proliferation of human umbilical vascular endothelial cells (24). Although it is not clear whether the *in vitro* proliferation of cultured endothelial cells reflects physiological vessel formation, our results do show that *Foxo1* is highly expressed in developing vessels.

The observation that *Foxo3a*$^{-/-}$ female mice have an age-dependent reduced fertility is interesting in light of the observations in *C. elegans* that *daf-16* mutations suppress all of the phenotypes of *daf-2* mutants, including reduced fertility (4). This finding may suggest that the role of Foxo3a in reproduction has been modified during evolution. Early and widespread initiation of follicular growth and subsequent early atretic change occurred by 9.5 weeks of age, followed by a noticeable absence of growing follicles. This is likely to be the primary cause of the observed age-dependent reduced fertility. These latter results are consistent with a recent report (25) that showed the dependence of follicular development on Foxo3a by using a different gene disruption approach. Ovarian follicular development is regulated by intragonadal factors and extragonadal factors (26). Intragonadal factors initiate follicular growing and coordinate development of the oocyte, granulosa cell, and thecal cell in the follicle at early stages. Extragonadal factors regulate granulosa cell and thecal cell function synchronously at later stage. Our results suggest that Foxo3a may have a suppressive effect on initiation of follicular growth by affecting the mechanisms intrinsic to the ovary, but further analyses including extragonadal factors such as FSH and LH are needed to support this hypothesis.

Initial screening of *Foxo4*$^{-/-}$ mice failed to detect an obvious phenotype. However, studies in *C. elegans* showed that the phenotype of *daf-16* mutants becomes more obvious under nonphysiological conditions, such as in combination with *daf-2* or *age-1* mutations (4). In fact, as described (18), we could identify the roles of Foxo1 in insulin metabolism by analyzing *Foxo1*$^{+/-}$ mice under conditions of abnormal insulin resistance. Thus, further analysis under a variety of conditions may yet reveal the physiological function for Foxo4.

A new Foxo family member, Foxo6, was reported recently (27). Interestingly, Foxo6 has several different characteristics when compared to the other Foxo family members, such as lack of some phosphorylation sites conserved in other members and predominant nuclear localization under serum or insulin stimulation. Whether Foxo6 participates in the regulation of cell cycle, apoptosis, metabolism, and stress responses is not yet known. Further study of Foxo6 both *in vitro* and *in vivo* will contribute to our understanding of the functional roles of the Foxo transcription factors.

The work described here represents the first step in determining essential roles for the Foxo family of transcription factors. Foxo1 clearly has an essential role in embryonic vascular development and Foxo3a a role in ovarian follicular physiology, whereas Foxo4, in this preliminary study, is seemingly nonessential. The diverse functions of the Foxo members demonstrated here may be due, at least in part, to differences in their transcriptional targets. Future work toward the identification of physiological targets specific to each Foxo family member, especially targets of Foxo1 in vascular development and targets of Foxo3a in the ovarian follicular development, will be crucial to our understanding of the various roles played by this family of transcription factors. Furthermore, by crossing the three mouse lines described here, insight can be gained into possible redundancy among these three Foxo family members.

We thank Dr. P. Soriano for providing the β-geo construct, Dr. C. MacLeod for help with ES cell culture, M. Paulus and the University of California at San Diego transgenic core for help with targeting and blastocyst injection, the University of California at San Diego histology core for histology preparation, and Dr. Arthur Sands and Lexicon Genetics for the Foxo3a targeted ES cells. This work was supported in part by National Institutes of Health National Research Service Award CA68672 and the National Foundation for Cancer Research.

1. Arden, K. C. & Biggs, W. H., III (2002) *Arch. Biochem. Biophys.* **403,** 292–298.
2. Lin, K., Dorman, J. B., Rodan, A. & Kenyon, C. (1997) *Science* **278,** 1319–1322.
3. Ogg, S., Paradis, S., Gottlieb, S., Patterson, G. I., Lee, L., Tissenbaum, H. A. & Ruvkun, G. (1997) *Nature* **389,** 994–999.
4. Tissenbaum, H. A. & Ruvkun, G. (1998) *Genetics* **148,** 703–717.
5. Biggs, W. H., III, Meisenhelder, J., Hunter, T., Cavenee, W. K. & Arden, K. C. (1999) *Proc. Natl. Acad. Sci. USA* **96,** 7421–7426.
6. Brunet, A., Bonni, A., Zigmond, M. J., Lin, M. Z., Juo, P., Hu, L. S., Anderson, M. J., Arden, K. C., Blenis, J. & Greenberg, M. E. (1999) *Cell* **96,** 857–868.
7. Kops, G. J., de Ruiter, N. D., De Vries-Smits, A. M., Powell, D. R., Bos, J. L. & Burgering, B. M. (1999) *Nature* **398,** 630–634.
8. Nakae, J., Park, B. C. & Accili, D. (1999) *J. Biol. Chem.* **274,** 15982–15985.
9. Burgering, B. M. & Medema, R. H. (2003) *J. Leukocyte Biol.* **73,** 689–701.
10. Tran, H., Brunet, A., Griffith, E. C. & Greenberg, M. E. (2003) *Sci. STKE* **2003,** RE5.
11. Anderson, M. J., Viars, C. S., Czekay, S., Cavenee, W. K. & Arden, K. C. (1998) *Genomics* **47,** 187–199.
12. Biggs, W. H., III, Cavenee, W. K. & Arden, K. C. (2001) *Mamm. Genome* **12,** 416–425.

13. Furuyama, T., Nakazawa, T., Nakano, I. & Mori, N. (2000) *Biochem. J.* **349,** 629–634.
14. Kitamura, T., Nakae, J., Kitamura, Y., Kido, Y., Biggs, W. H., III, Wright, C. V., White, M. F., Arden, K. C. & Accili, D. (2002) *J. Clin. Invest.* **110,** 1839–1847.
15. Nakae, J., Kitamura, T., Kitamura, Y., Biggs, W. H., III, Arden, K. C. & Accili, D. (2003) *Dev. Cell* **4,** 119–129.
16. Richards, J. S., Sharma, S. C., Falender, A. E. & Lo, Y. H. (2002) *Mol. Endocrinol.* **16,** 580–599.
17. Bois, P. R. & Grosveld, G. C. (2003) *EMBO J.* **22,** 1147–1157.
18. Nakae, J., Biggs, W. H., III, Kitamura, T., Cavenee, W. K., Wright, C. V., Arden, K. C. & Accili, D. (2002) *Nat. Genet.* **32,** 245–253.
19. Zambrowicz, B. P., Friedrich, G. A., Buxton, E. C., Lilleberg, S. L., Person, C. & Sands, A. T. (1998) *Nature* **392,** 608–611.
20. Finch, R. A., Donoviel, D. B., Potter, D., Shi, M., Fan, A., Freed, D. D., Wang, C. Y., Zambrowicz, B. P., Ramirez-Solis, R., Sands, A. T. & Zhang, N. (2002) *Cancer Res.* **62,** 3221–3225.
21. Hogan, B., Beddington, F., Constantini, F. & Lacy, E. (1994) *Manipulating the Mouse Embryo: A Laboratory Manual* (Cold Spring Harbor Lab. Press, Woodbury, NY).
22. Pedersen, T. & Peters, H. (1968) *J. Reprod. Fertil.* **17,** 555–557.
23. Jain, R. K. (2003) *Nat. Med.* **9,** 685–693.
24. Potente, M., Fisslthaler, B., Busse, R. & Fleming, I. (2003) *J. Biol. Chem.* **278,** 29619–29625.
25. Castrillon, D. H., Miao, L., Kollipara, R., Horner, J. W. & DePinho, R. A. (2003) *Science* **301,** 215–218.
26. Elvin, J. A. & Matzuk, M. M. (1998) *Rev. Reprod.* **3,** 183–195.
27. Jacobs, F. M., Van Der Heide, L. P., Wijchers, P. J., Burbach, J. P., Hoekman, M. F. & Smidt, M. P. (2003) *J. Biol. Chem.* **278,** 35959–35967.